Physica B 404 (2009) 2795–2798

Contents lists available at ScienceDirect

Physica B

journal homepage: www.elsevier.com/locate/physb

Effect of catalyst preparation on the yield of carbon nanotube growth

Mariano Escobar [a,b,*], Gerardo Rubiolo [c,d], Roberto Candal [d,e], Silvia Goyanes [b,d]

[a] Dep. Química Inorgánica, Analítica y Química Física, FCEyN, UBA, Ciudad Universitaria (1428), Bs As, Argentina
[b] LP&MC, Dep. Física, FCEyN, UBA, Argentina
[c] Unidad de Actividad Materiales, CNEA, Av Gral Paz 1499, San Martin (1650), Bs As, Argentina
[d] Consejo Nacional de Investigaciones Científicas y Técnicas (CONICET), Argentina
[e] Instituto de Físico-química de Materiales, Ambiente y Energía (INQUIMAE), CONICET – UBA, Argentina

ARTICLE INFO

Keywords:
Carbon nanotubes
Sol gel
Catalysis

ABSTRACT

Multi-wall carbon nanotubes (MWCNTs) were synthesized by catalytic chemical vapor deposition (CVD) on catalytic iron nanoparticles dispersed in a silica matrix, prepared by sol gel method. In this contribution, variation of gelation condition on catalyst structure and its influence on the yield of carbon nanotubes growth was studied. The precursor utilized were tetraethyl-orthosilicate and iron nitrate. The sols were dried at two different temperatures in air (25 or 80 °C) and then treated at 450 °C for 10 h. The xerogels were introduced into the chamber and reduced in a hydrogen/nitrogen (10%v/v) atmosphere at 600 °C. MWCNTs were formed by deposition of carbon atoms from decomposition of acetylene at 700 °C. The system gelled at RT shows a yield of 100% respect to initial catalyst mass whereas the yield of that gelled at 80 °C was lower than 10%. Different crystalline phases are observed for both catalysts in each step of the process. Moreover, TPR analysis shows that iron oxide can be efficiently reduced to metallic iron only in the system gelled at room temperature. Carbon nanotubes display a diameter of about 25–40 nm and several micron lengths. The growth mechanism of MWCNTs is base growth mode for both catalysts.

1. Introduction

One of the most promising ways for large scale CNT production is chemical vapor deposition (CVD). Using this technique, different supports (alumina, silica, magnesium oxide) were investigated to determine their effects on the size of the metal nanoparticles and on the diameter and structural characteristics of carbon nanotubes [1].

Sol gel technology provides an excellent way to obtain catalyst nanoparticles to synthesize multi-wall carbon nanotube. The porous nature of the matrix formed by sol–gel provides the sites for nucleation of the iron oxide particles, minimizes their aggregation, and imposes an upper limit on their size [2].

Yu et al. [3] reported a relationship between an optimum catalyst particle size and maximum growth rate using a series of silica supported iron catalyst.

Perez Cabero et al. [4] found that the iron precursor utilized and the preparation conditions of the silica supported catalysts have a high influence on the final reaction yield and on the characteristics of the carbon products obtained. Recently, Perez Cabero et al [5] have optimized this method getting a yield of 30 wt% of CNT over iron–silica catalysts.

In this contribution, variation of gelation condition on catalyst structure and its influence on the yield of carbon nanotubes growth was studied.

2. Experimental

Tetraethyl ortho silicate (Aldrich) (5 ml) was mixed with 0.9 M iron nitrate (Riedel de Hagen) aqueous solution (7.5 ml) and ethanol (10 ml) by magnetic stirring for 20 min. A few drops of concentrated hydrogen fluoride (0.4 ml) were then added, and the mixture was stirred for another 20 min. The mixture was then dropped onto a borosilicate glass plate. Gelation and xerogel formation process were carried out at two temperatures: 25 °C (catalyst #1) and 80 °C (catalyst #2). After that, the substrates were fired at 450 °C for 10 h in air and then reduced at 600 °C for 5 h in a flow of 10% hydrogen in nitrogen at 180 Torr. Finally, 3 sccm of acetylene diluted in 107 sccm of nitrogen (2.5% of acetylene in nitrogen) were introduced into the chamber with a flow rate of 110 cm^3/min. During this step, carbon nanotubes were formed on substrates by deposition of carbon atoms from decomposition of acetylene at 700 °C under 180 Torr. The growth

* Corresponding author at: Dep. Química Inorgánica, Analítica y Química Física, FCEyN, UBA, Ciudad Universitaria (1428), Bs As, Argentina.
Tel.: +54 11 4576 3300x255; fax: +54 11 4576 3357.
E-mail address: mescobar@df.uba.ar (M. Escobar).

0921-4526/$ - see front matter Crown Copyright © 2009 Published by Elsevier B.V. All rights reserved.
doi:10.1016/j.physb.2009.06.088

time was 3 h. After that, the furnace was cooled to the room temperature under flowing nitrogen gas.

X-ray diffraction patterns (XRD) were recorded for substrates at different synthesis stages. X-ray diffractometer Siemens D5000, with Cu-Kα radiation and a graphite monochromator was employed. Temperature-programmed reduction (TPR) experiments were carried in a thermobalance (Shimadzu TGA-51), using a gas mixture 10% of Hydrogen in Nitrogen. Thermogravimetric Analysis (Shimadzu TGA-51) and Differential Thermal Analysis (Shimadzu DTA-50) were performed on 15 mg catalysts with a heating rate of 10 K/min and air flow (50 cm^3/min). Transmission electronic microscopy (TEM-EM Philips 301) was employed to study the different morphologies.

3. Results and discussion

XRD spectra for the catalyst #1 and #2 fired at 450 °C for 10 h are presented in Fig. 1. The catalyst #1 show well defined peaks, clearly assigned to α-Fe_2O_3, Also, it presents a typical broad feature due to amorphous silica present at 23–27°. Catalyst #2 display broad and poor defined peaks, which can be assigned to the same crystalline structure. Clearly, the cristallinity of iron oxide in catalyst #2 is much lower than in # 1, suggesting that the iron oxide is highly dispersed in the silicon dioxide matrix. However, it can also be assigned to hematite.

This can be explained taking into account that the time required to eliminate the solvents is longer for catalyst #1. This situation favor the migration of Fe(III) and the formation of larger iron oxide nuclei that, after thermal treatment, lead to larger and crystalline particles.

The solvents presents in Catalyst #2 is eliminated quickly, so Fe(III) remain well dispersed in the silica matrix favoring the formation of iron silicate.

The catalysts undergo successive phase's transformations during CNT synthesis process. Fig. 2 shows the derivative temperature programmed reduction (TPR) curve. It can be seen that several transformations take place as the temperature increases from 25 to 900 °C under reductive atmosphere.

The sequence of such transformations can be resumed as: water loss, $Fe_2O_3 \rightarrow Fe_3O_4$, $Fe_3O_4 \rightarrow FeO$, and $FeO \rightarrow Fe$. The derived TPR curve is located at about 80, 370–430, 600–650, and 650–850 °C. The continuous weight loss at 900 °C is assigned to the reduction of silicate species [3]. Catalyst #2 does not present the later transformation ($FeO \rightarrow Fe$), but it shows a strong peak, about 160 °C corresponding to release of adsorbed water.

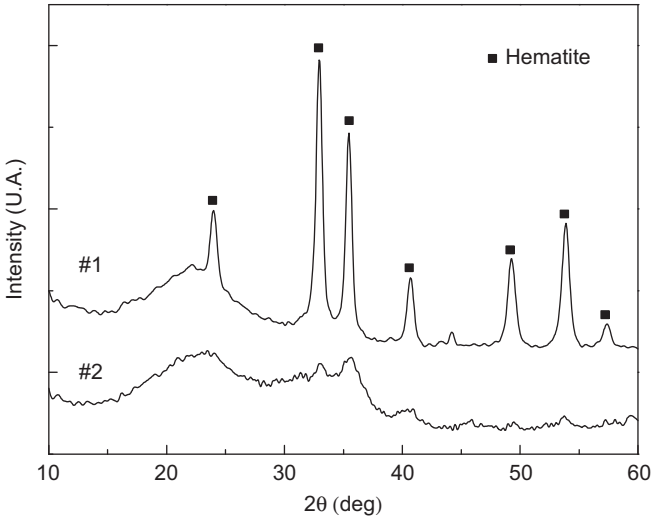

Fig. 1. XRD patterns of catalysts fired at 450 °C in air.

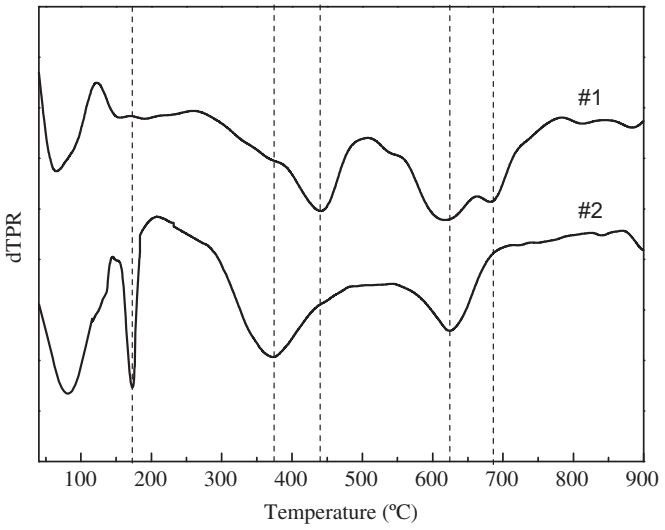

Fig. 2. Derivate TPR profiles of both catalysts.

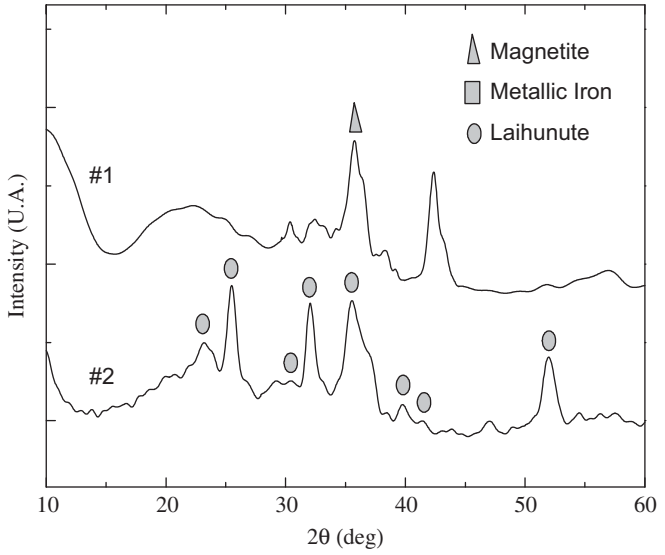

Fig. 3. XRD patterns of catalysts after reduction treatment.

Fig. 3 shows XRD results corresponding to reduced catalysts. Catalyst #1 presents a well defined crystalline structure which can be assigned to magnetite, with a typical feature at 35°. It can also be observed a peak at 43° corresponding to metallic iron. Catalyst #2 presents a pattern of iron silicate, laihunite. This reaction between iron oxide and silica matrix could be favoured by the fine distribution of Fe (III) dispersed in the matrix.

Fig. 4 shows XRD pattern of catalysts after decomposition of acetylene. The observed crystalline structure corresponds to an iron silicate named fayalite in both systems; however, the degree of crystallinity is higher in the catalyst #2. This transformation of laihunite to fayalite involves the reduction of all the Fe(III) present in laihunite to Fe(II) due to the reductive character of the N_2-acetylene mixture. It is interesting that catalyst #1 pattern shows a MWCNT (multi-wall carbon nanotube) peak.

Thermogravimetric analysis results are presented in Fig. 5. There is a slight increase of the mass until 350 °C due to incorporation of oxygen to the catalysts. Catalyst #2 shows a weight loss of about 5% in the range 350–450 °C due to

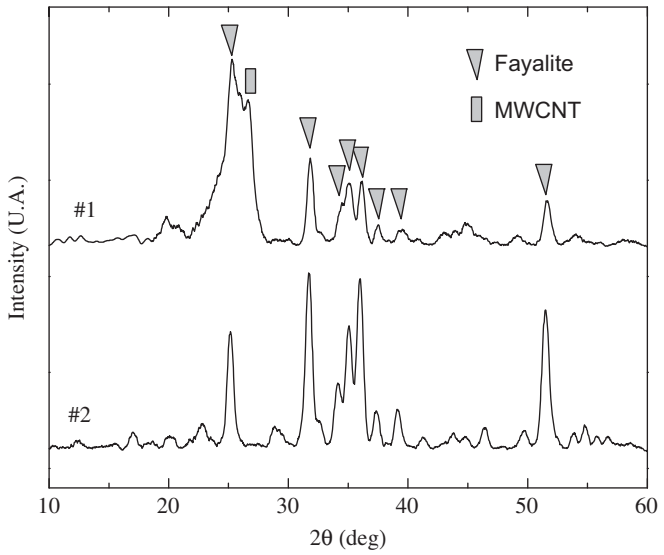

Fig. 4. XRD patterns of catalysts after carbon deposition.

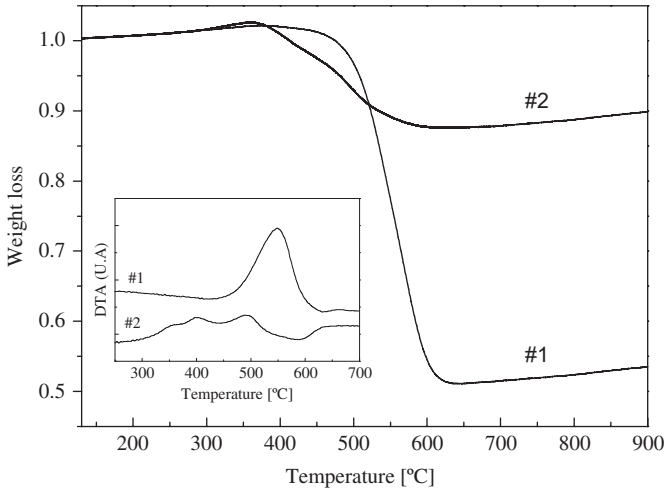

Fig. 5. TGA and DTA (inset) of catalysts after carbon deposition.

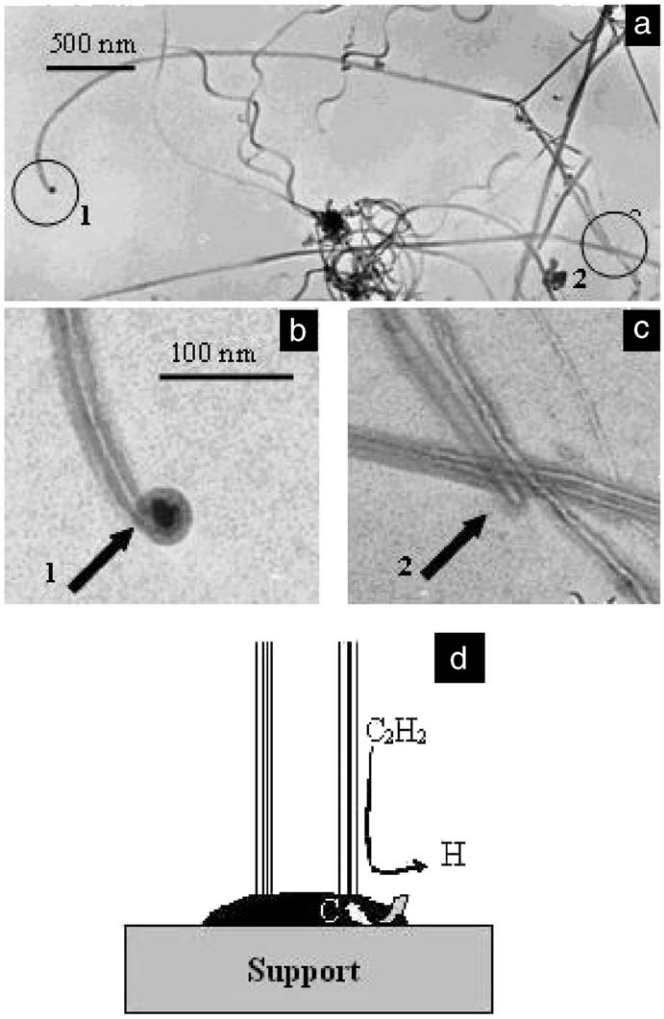

Fig. 6. TEM images of MWCNT obtained with catalyst #1 (a–c) and scheme of growth mechanism (d).

elimination of amorphous carbon. Degradation of carbon nanotubes occurs in the range of 450–600 °C, with a weight loss of 7%. Catalyst #1 shows a weight loss in the range of 480–600 °C corresponding to the degradation of carbon nanotubes; there is not indication of the presence of amorphous carbon. DTA results confirms clearly the elimination of amorphous carbon at 350–400 °C in catalyst #2 and the peak at 500 °C corresponds to the degradation of carbon nanotubes. Catalyst #1 shows a maximum located approximately at 550 °C due to MWCNTs degradation (inset Fig. 5). Thermal analysis lead to the following conclusions: MWCNTs obtained from catalyst #1 present a higher degree of crystallinity and MWCNTs obtained from catalyst #2 have a lot of impurities, i.e. amorphous carbon.

Due to the amount of catalyst as well as growth condition were the same in CVD process for both catalysts, the efficiency of each one to produce MWCNTs can be deduced from TGA results. Regarding Catalyst #2, about 12 wt% of the initial mass corresponds to carbonaceous material (5% to amorphous carbon and 7% to MWCNTs) while catalyst #1 presents about 50 wt% of initial mass corresponding to carbonaceous structures (100% of MWCNTs). The reason can be found in TPR and XRD results: catalyst #1 has a great amount of metallic iron present at the moment of carbon deposition. Catalyst #2 should also have a minimal percentage of metallic iron but it is not detectable by TPR and XRD. Therefore, it would be expected that the yield was higher than in the case of catalyst #2.

Fig. 6 shows TEM images of MWCNTs obtained from both catalysts. Fig. 6a shows a low magnification micrograph of MWCNT from catalyst #1. The two ends of a single carbon nanotube can be seen in this picture (circles 1 and 2). An amplified image (Fig. 6b and c) indicates that one extreme have an iron nanoparticle inside of the carbon structure and the other is closed with a fullerene-like structure, in concordance with several works [1,6,7]. Due to nanoparticle diameter is higher than that of nanotube (42 versus 32 nm, respectively), it could be concluded that the growth mechanism is base mode, as is indicated in Fig. 6d. MWCNTs obtained from catalyst #2 present similar characteristics regarding diameter and growth mechanism.

4. Conclusion

Multi-wall carbon nanotubes were synthesized using iron nanoparticles dispersed in a silica matrix as catalyst. Variations on the drying temperature in sol gel process have a strong influence on the morphology and crystallinity of iron oxide nanoparticles and on the catalytic activity for MWCNTs production. The high yield of carbon nanotube production is a consequence of the

higher proportion of metallic iron in catalyst #1; the iron–silica interaction and the presence of iron silicate seems to have an important role in the yield of the process.

Acknowledgments

This work was supported by Universidad de Buenos Aires, Argentina (Investigation Project, X191); Consejo Nacional de Investigaciones Científicas y Técnicas (PIP 5215; PIP 5959) and Agencia Nacional de Promoción Científica y Tecnológica (PICT 10-25834 and PICT 06-10621).

References

[1] A. Dupuis, Progress in Materials Science 50 (2005) 929.
[2] F. Del Monte, M. Morales, D. Levy, A. Fernandez, M. Ocan, A. Roig, E. Molins, C. Serna, Langmuir 13 (1997) 3627.
[3] Z. Yu, D. Chen, B. Tøtdal, A. Holmen, Catalysis Today 100 (2005) 261.
[4] M. Pérez-Cabero, A. Monzón, I. Rodriguez-Ramos, A. Guerrero-Ruiz, Catalysis Today 93 (2004) 681.
[5] F.R. García-García, M. Pérez-Cabero, D.M. Nevskaia, I. Rodríguez-Ramos, A. Guerrero-Ruiz, Catalysis Today 133 (2008) 815.
[6] Z.W. Pan, S.S. Xie, B.H. Chang, L.F. Sun, W.Y. Zhou, G. Wang, Chemical Physics Letters 299 (1999) 97.
[7] M. Pérez-Cabero, I. Rodríguez-Ramos, A. Guerrero-Ruiz, Journal of Catalysis 215 (2003) 305.